knowledge

MDPI

Article

SmartLabAirgap: Helping Electrical Machines Air Gap Field Learning

Carla Terron-Santiago †, Javier Martinez-Roman *,†, Jordi Burriel-Valencia † and Angel Sapena-Bano †

Institute for Energy Engineering, Universitat Politècnica de València, Camino de Vera s/n, 46022 Valencia, Spain; cartersa@upvnet.upv.es (C.T.-S.); jorburva@die.upv.es (J.B.-V.); asapena@die.upv.es (A.S.-B.)

* Correspondence: jmroman@die.upv.es

† All authors contributed equally to this work.

Abstract: Undergraduate courses in electrical machines often include an introduction to the air gap magnetic field as a basic element in the energy conversion process. The students must learn the main properties of the field produced by basic winding configurations and how they relate to the winding current and frequency. This paper describes a new test equipment design aimed at helping students achieve these learning goals. The test equipment is designed based on four main elements: a modified slip ring induction machine, a winding current driver board, the DAQ boards, and a PC-based virtual instrument. The virtual instrument provides the winding current drivers with suitable current references depending on the user selected machine operational status (single- or three-phase/winding with DC or AC current) and measures and displays the air gap magnetic field for that operational status. Students' laboratory work is organized into a series of experiments that guide their achievement of these air gap field-related abilities. Student learning, assessed based on pre- and post-lab exams and end-of-semester exams, has increased significantly. The students' opinions of the relevance, usefulness, and motivational effects of the laboratory were also positive.

Keywords: electric engineering education; practice-based theory development; magnetic field measurement; students experiments; test equipment

check for updates

Citation: Terron-Santiago, C.; Martinez-Roman, J.; Burriel-Valencia, J.; Sapena-Bano, A. SmartLabAirgap: Helping Electrical Machines Air Gap Field Learning. *Knowledge* **2024**, *4*, 382–396. https://doi.org/10.3390/knowledge4030021

Academic Editor: Jose María Merigo

Received: 2 May 2024
Revised: 3 July 2024
Accepted: 8 July 2024
Published: 11 July 2024

Copyright: © 2024 by the authors. Licensee MDPI, Basel, Switzerland. This article is an open access article distributed under the terms and conditions of the Creative Commons Attribution (CC BY) license (https://creativecommons.org/licenses/by/4.0/).

1. Introduction

The air gap magnetic field (AMF) of rotating electrical machines is a fundamental magnitude to describe machine performance, as it directly influences the windings' induced electromotive force (EMF) and the machine torque. Introductory courses on electrical machines often analyze the AMF produced by windings with different structures and excitations (DC and single- and three-phase AC), e.g., [1–4].

Engineering degree students often face significant challenges when learning electromagnetism and electrical machines due to the use of abstract concepts that are hard to visualize [5,6] and to the lack of appropriate measurement equipment and test rigs. At the very foundation of the energy conversion in rotating electrical machines lies the interaction between the stator and rotor air gap magnetic fields. These two fields must rotate at the same velocity for a net average torque to be developed. Two experiments to reinforce these concepts were introduced in [7]. In this work, an analog oscilloscope was used to obtain the changes in the induced EMF on the rotor windings. Also, configurable winding electrical machines with search coils have long been used to in electrical machine laboratories to indirectly measure the air gap flux density. However, these set-ups are very cumbersome and usually require some level of oscilloscope operation mastery that cannot often be expected of early learners of electrical machines. The use of search coils to measure the AMF of a synchronous generator instead of the more usual phase-related measurements was shown in [8] to provide better insight into the energy conversion process. A cost-effective solution based on simulation tools has also been adopted, as shown in [9,10]. More recently,

it has been applied to the broader framework of electrical machines and drives in [11–13]. A combination of mechanical, electrical, and computer engineering has also been applied to the comprehensive technological discipline of robotics [14]. However, one should also consider the drawbacks of simulated systems, such as the time needed for students to become familiar with them or the perception among students that they are of limited helpfulness [15]. This limitation is also explicitly pointed out in [16,17]. The teaching of science, technology, and engineering still lags behind in adopting new technological approaches, mainly because these fields often require laboratory exercises to provide effective skill acquisition and hands-on experience. On the other hand, similar difficulties arise already at the undergraduate level [18], where it has been shown that augmented reality is more effective than web-based learning in promoting students' understanding of electromagnetic concepts and phenomena.

Smart labs (SLs) are made up of the combination of a transducer/actuator board, a digital acquisition (DAQ) board, and a computer and application-specific software (DAQ control, acquired data manipulation and handling and user interface). This last element is often referred to as the virtual instrument (VI), using the widespread terminology of DAQ boards and development software manufacturers [19]. SLs often include the actual equipment undergoing testing, which is set to different operating conditions (using actuators that are driven or not by the same SL). Its performance is measured, processed, and displayed to the user by the VI. SLs must not be confused with simulated systems. They have been shown to offer many advantages over traditional setups. As early as 1984, reference [20] already demonstrated the suitability of SLs in helping students obtain a 'real-time' handle on some electrical machines concepts such as 'live' phasor diagrams of a synchronous machine under different torque and excitation conditions. Efficient data collection and manipulation using VIs is shown in [21] to help maintain student interest and reduce the time required to perform and evaluate experiments. Similar advantages have been reported in [22]. The VI's ability to provide a friendly interaction between the student and the experiment is also highlighted in [23]. The modular and reusable nature of SLs, and therefore their suitability to be integrated into cost-effective systems, is highlighted in [24]. The additional benefits introduced by the collaboration of students in the development of SLs, namely that the SL reflect their interests and needs, among the other advantages already mentioned, have also described in [25]. Other applications of SLs to the study of rotating electrical machines and drives can be found, for example, in [26–29].

The Electrical Machines course at the Escuela Técnica Superior de Ingenieros Industriales, Universitat Politècnica de València has about 500 students enrolled in Industrial Technologies (GITI) and Energy (GIE) engineering degrees, as well as the Industrial Engineering Master's program (MII). The course curriculum includes magnetic circuits (10%), transformers (45%), and rotating electrical machines (REM, 45%). Regarding REM, the former lab was devoted to perform and analyze the locked rotor, no-load (with loss segregation), and load tests of induction machines (IM). Due to the challenges students face in understanding the air gap magnetic field (AMF) waves produced by different winding structures and excitations, this laboratory will be enhanced to visually demonstrate the AMF produced by full-pitch coils, pitched coils, and typical distributed windings under various current excitations, including DC and single- and three-phase AC. The primary goal is to enhance the student experience, making it easier for them to grasp and consolidate complex and abstract concepts such as the magnetic field in the air gap of a rotating electrical machine. This virtual laboratory allows students to quickly and visually observe the magnetic field distribution in a real machine under different conditions, such as varying combinations of DC or AC currents and different stator winding configurations. Through this experience, students can observe the transformation of the field from a constant field (supplied by DC) to a pulsating field (supplied by a single-phase AC) and, ultimately, to a rotating field (desired in three-phase machines). Additionally, they can see how the amplitude and frequency of the current, which they can modify, affect the amplitude and pulsation speed (in single-phase excitation) and the rotational speed of the field (in

three-phase excitation). This, in turn, shows the impact on the rotation of the rotating electrical machine. Moreover, the virtual lab enables students to visualize these concepts in both electrical and mechanical angles, addressing another challenging topic for learners. They can explore the real magnetic field wave, including all its harmonics (such as slotting and distribution), or they can focus on only the main harmonic, which is traditionally used to explain the magnetic field in the air gap of the machine. Typically, the analysis is simplified by assuming a constant air gap amplitude, which is not the case in reality. The proposed session tasks allow students to observe the subtle variations caused by the actual stator winding configuration, the real air gap, slotting, and other factors. Ultimately, this improvement in the lab session aims to aid students in understanding fundamental REM concepts, thereby enhancing their learning and increasing their motivation to study electrical machines.

This paper first states the pursued objectives in Section 2. Then, Section 3 describes the design process that is followed to develop the new SmartLabAirgap test equipment and the associated instructional guide with the aim of fulfilling the pursued objectives. The impact of the lab on the students' learning, motivation, and opinions on the relevance and usefulness of the lab are evaluated in Section 4. Finally, the main conclusions of this work are presented in Section 5.

2. Objectives

The general objective pursued within the framework of this project was to develop a tool that could help in improving the students' understanding of the complex relationships between winding structure, excitation, and AMF characteristics including amplitude, orientation, and rotational speed. Traditionally, methods to explain this phenomenon have been based on the presentation of figures or two-dimensional drawings, where the representations of phasor diagrams are very abstract. Moreover, these are simplifications that do not consider the other effects that the proposed simulator allows the students to observe, such as the real air gap field wave with all its harmonics and the effects of changes in the air gap amplitude (slot), among others.

Therefore, to address this problem, the magnetic excitation introduced by a winding in the air gap can be accounted for in terms of the winding current sheet (WCS), as shown in Equation (1) :

$$a(\alpha, t) = n(\alpha) i(t) \cong \begin{cases} 0 \ ; \ no\, winding \\ \frac{\pm N_k\, i(t)}{\Delta}; \ winding\, slot\, k \end{cases} \tag{1}$$

where $n(\alpha)$ is the local winding conductor linear density, $N_{(k)}$ is the number of winding conductors in the winding slot k, $i(t)$ is the winding current, and Δ is the slot opening width. Let us consider a constant and small air gap (δ) and a machine with very high iron permeability. Neglecting the iron mmf drop, the AMF can be derived from the air gap current sheet, as shown in Equation (2):

$$\frac{\partial B(\alpha, t)}{\partial \alpha} = \frac{\mu_0}{\delta} \frac{D}{2} a(\alpha, t) \tag{2}$$

This describes the relationship between the AMF wave and the winding structure and current through the WCS wave. Thus, a single winding produces stationary WCS and AMF waves with a constant (DC current) or pulsating (AC current) amplitude. The equivalence between a pulsating stationary wave and two traveling waves with half its amplitude traveling at a constant speed (or with the same period of the stationary wave) but in opposite directions is sometimes used as the starting point to deduce the rotating nature of the AMF produced by a three-phase symmetrical winding excited by three-phase balanced currents [3]. This rotating nature of the fundamental AMF can also be deduced from the addition of the fundamental AMF waves produced by each one of the three-phase windings, as in [1,2,4], when excited by a balanced three-phase current system. The

angular frequency of this rotating AMF wave, Ω, is directly related to the current's angular frequency, ω, through the machine's pole number, P .

$$\Omega = \frac{2}{P}\omega \tag{3}$$

Taking these concepts into account, the general objective just presented can be divided into simpler ones; that is, a tool that could help to:

- Differentiate between stationary—either with a constant or pulsating amplitude—and rotating AMF,
- Correlate each kind of AMF with the winding excitation (DC and single- or three-phase AC),
- Link different AMF waveforms to the winding structure required to produce them,
- Contrast the classic and widespread Cartesian representation of the AMF with the actual cylindrical air gap,
- Recognize the distinction between the AMF waveform and the angular frequencies of the winding currents in multipolar machines,
- Motivate the students by helping them bridge the gap between the analytical tools used to describe the AMF wave and its perceived effect on the machine performance,
- Reduce the time taken to mature these concepts.

3. SmartLabAirgap

New laboratory test equipment was developed to help the students correlate the basic winding configuration characteristics and the different excitation options with the properties of the AMF: the SmartLabAirgap (SLA). The first premise for the SLA design was *'measuring is believing'*. Thus, the first design choice was to design and create a tool to generate and measure the actual AMF inside a real rotating electrical machine instead of a simulation tool.

3.1. AMF Measurement

To measure the actual AMF inside a real rotating electrical machine, an indirect measurement using a search coil made up of two active conductors set π rad (electrical) apart was chosen due to the ease of installation within the electrical machine air gap compared to Hall effect magnetic field transducers. The search coil-induced EMF is proportional to the AMF at the search coil position, $B(\theta_c)$, and to the angular velocity at which it rotates relative to the coil, Ω, as shown in Equation (4):

$$e_{searchoil}(t) = 2B(\theta_c)l\frac{D}{2}\Omega \tag{4}$$

where l is the stack length and D is the air gap diameter. Measuring the AMF indirectly with a search coil introduces two new problems: how to connect the rotating search coil to the stationary measuring equipment and how to correlate the EMF time waveform to the AMF angular waveform. To solve the first one, the classic slip ring/brush arrangement was favored over more complex wireless transmission systems. To keep costs low by avoiding the installation of new slip rings and brushes, a fractional HP slip ring induction machine was chosen. The original three-phase rotor winding of the slip ring induction machine was disconnected from the slip rings. Then, two full pitch search coils, glued in four specifically milled straight superficial slots 90° (electrical) apart, were connected as shown in Figure 1 (although only one search coil is needed to indirectly measure the AMF, as there were three slip rings available, a second one was installed for redundancy).

To correlate the induced EMF time waveform with the AMF angular waveform, any angular position transducer can be used to report the search coil position ϑ_c to the measurement system, along with the induced EMF $e(t)$, so that $B(\vartheta_c)$ can be computed using Equation (4). An optical incremental encoder was selected due to the high noise immunity and the widely available encoder or counter inputs in DAQ cards. A small four pole induction machine already available in the lab was coupled to the slip ring induction

machine to drive it almost to its synchronous speed of 1500 r/min with a 50 Hz mains frequency.

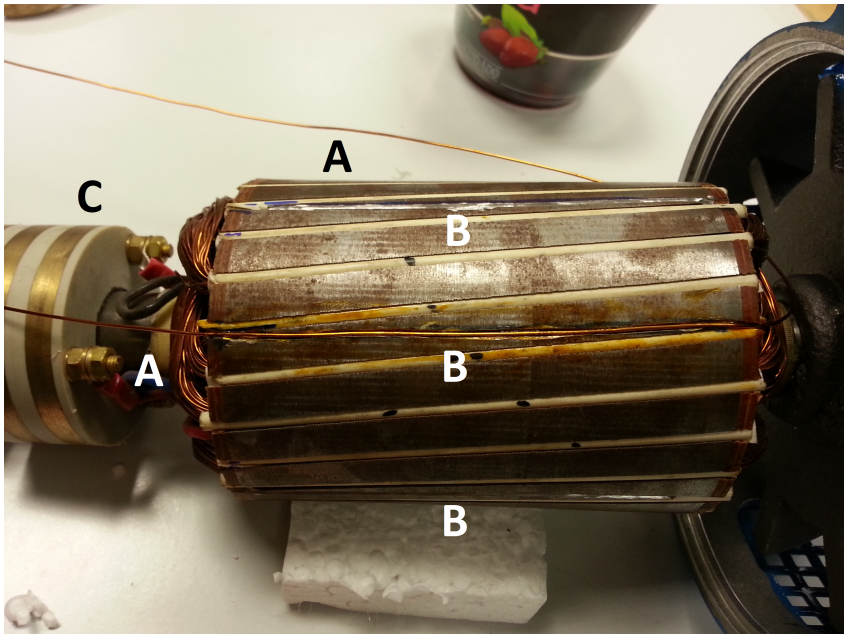


Figure 1. Search coils (A) installed in the new milled straight superficial slots (B) and to be connected to the original rotor slip rings (C).

3.2. AMF Excitation

The SLA needed to provide the means to drive several windings with different structures independently or jointly with DC and single and three-phase AC currents. This was paramount to allow the user to explore the AMF produced by different winding structures and current excitations.

In terms of the winding structure, off-the-shelf three-phase machines have three phases with the same structure and are not directly suitable to this end. In particular, the slip ring induction machine, the one selected to make use of the already installed slip ring/brush, had three symmetrical phase windings, each one made up of three concentric coils per pole pair, with 66 turns per coil. To provide the ability to experiment with the SLA gradually using more complex windings, one of the phase windings was removed and rebuilt as a set of three independent coils (W1, W2, and W3, Figure 2) with the original turns. This way, the AMF produced by a single full-pitch coil (W1), two pitched coils (W23), a distributed winding with three slots per pole (phases U and V), and a typical three-phase symmetrical winding (phases U, V and W) could be explored.

In terms of the winding currents, each winding had to be driven by either DC or single or three-phase AC currents. Resorting again to the 'measuring (and seeing) is believing' motto of the SLA, the use of the AC mains frequency of 50 or 60 Hz was out of the question, as the relatively slow response of the human eye cannot distinctively perceive the comparatively fast effects associated with such high frequencies. To allow the SLA user to distinguish the details of the time evolution of the AMF, a far lower frequency range of 0.05 to 0.2 Hz (with large associated periods lying between 5 and 20 s) was selected. The use of a relatively wide frequency interval with a ratio of four between the largest and the smallest frequency was chosen to help the user recognize the link connecting the current frequency and AMF pulsating or angular frequencies.

Once it was decided that either DC or very low frequency AC current had to be driven to the four independent windings (U, V, W1, and W23) the problem became very similar, as at such low AC frequencies, the winding inductive effect is almost negligible compared to the resistive voltage drop, and many adjustable voltage sources would have been suitable. The first design decision was to use PC-based oscillators instead of electronic

oscillators; a task that fits well with the data processing and user interface still to be defined. To further simplify the whole set-up, instead of using bulky off-the-shelf programmable power supplies, a set of four power operational amplifiers, OPA544, were chosen and set up with a constant gain inverter amplifier configuration resulting in a quite compact design (Figure 3).

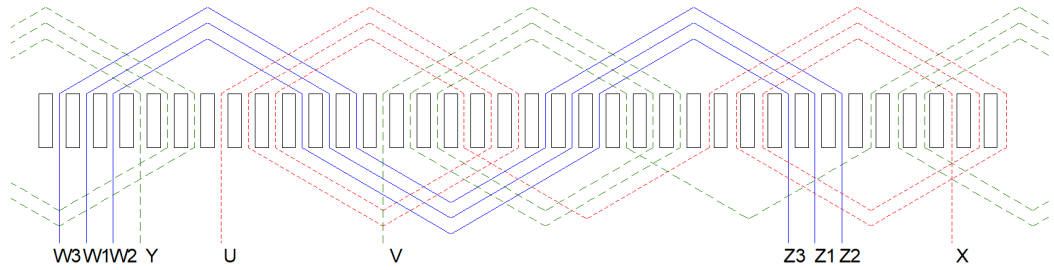


Figure 2. Three-phase symmetrical winding with three slots per pole per phase, rebuilt in one phase to split into one full-pitch coil and two short-pitched coils.

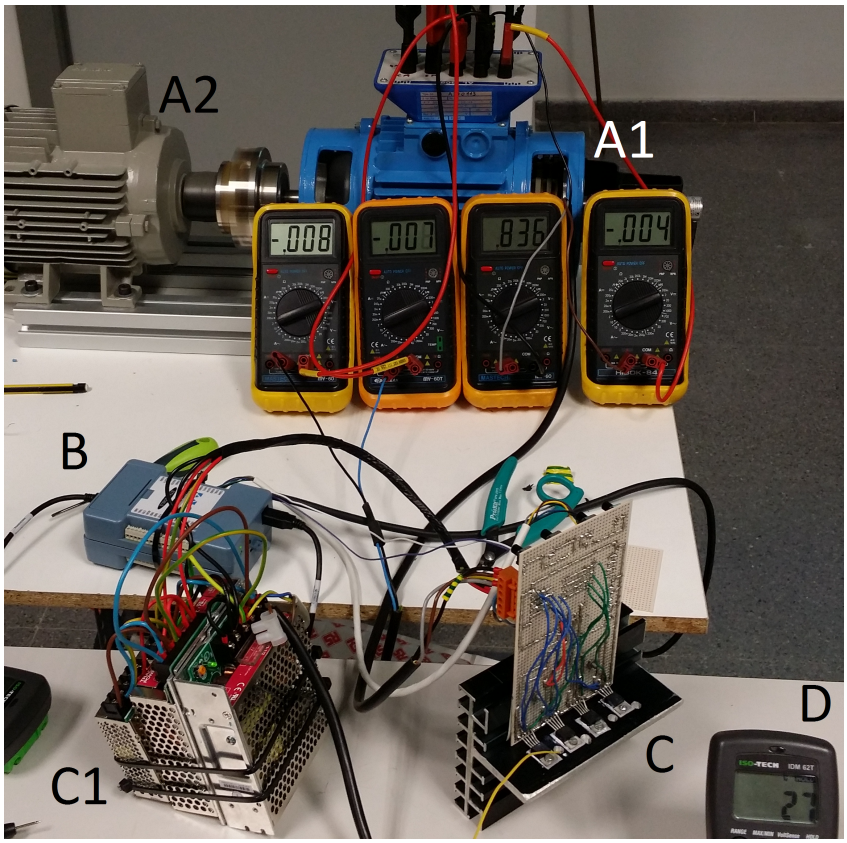


Figure 3. SmartLabAirgap setup (development stage). (A1) Main motor with custom stator phase windings and rotor search coils. (A2) Auxiliary motor. (B) DAQ cards. (C) Current drivers. (C1) Quad power supply. (D) OPA case temperature monitoring.

The technical specifications of each component of the set-up are specified below:

- Slip ring IM: 370 W rated power, 380/230 V, 1.2 A, 1390 rpm.
- Winding current driver board: based on OPA544 high-voltage, high-current operational amplifier, with 2 A rated current and up to ±35 V supply voltage.
- DAQ boards: BTH-1208-ls with eight single-ended AD channels with an 11 bit resolution and up to 47 kS/s, two DA channels with a 12 bit resolution, and eight programmable DIO units.

- PC-based VI: developed on Labview 2014 and runs on a Core i5/8 GB RAM/256 GB SSD /Windows 10 personal computer.

Figure 4 shows part of the set-up in its final enclosure in detail, where A corresponds to the DAQ cards, B marks the current drivers, and C shows the current divers' power supply. The materials cost of the equipment was roughly 4000 EUR, provided the institution had a valid a Labview license. This amount did not include the know-how, which might amount to approximately the same. To pluralize the experience, a simulation software that can be licensed based on actual measurements taken using this test equipment was developed. Although the experience was not the same as for the actual rotating machine, it conveys the same information regarding the actual rotating machine air gap field.

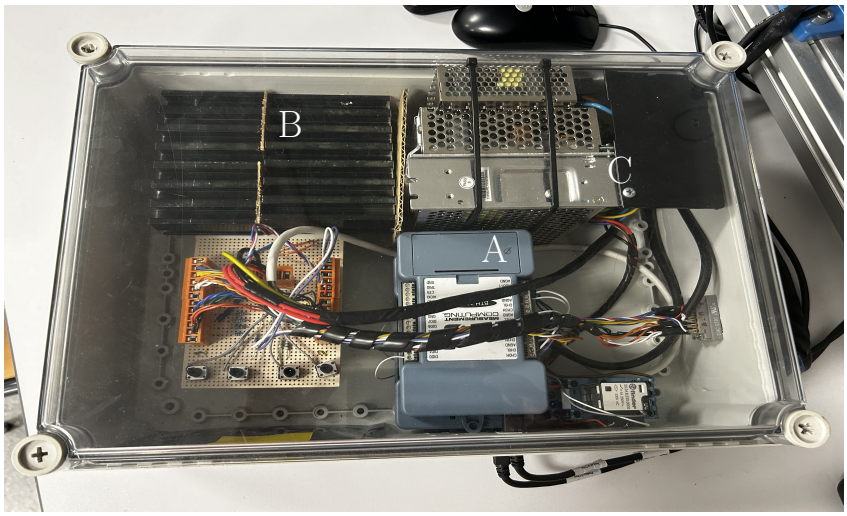


Figure 4. SmartLabAirgap setup detail. (A) DAQ cards. (B) Current drivers. (C) Quad power supply.

3.3. Measurement and Operation Interface

At this point, a suitable interface had to be selected in terms of analog-to-digital (AD) and digital-to-analog (DA) capabilities. The main AD constraint was to achieve enough angular resolution in the indirect AMF measurement, equivalent to the time resolution of the search coil-induced EMF. Thus, to reach at least 360 points per AMF or EMF period with a four-pole machine rotating at close to 1500 rpm and an EMF period of 20 ms, the lowest sampling frequency required was $f_{s,min}$ = 18 kS/s. In case of a mains frequency of 60 Hz and a rotor speed of 1800 rpm, this value rose to 21.6 kS/s; thus, f_s = 25 kS/s was chosen.

Along with the EMF, the encoder Z signal had to be measured for the time/angle correlation; thus, an aggregated $f_{s,agr}$ = 50 kS/s was required. With regard to the current drivers set points, a less strict resolution of at least 50 points per current period was deemed sufficient to provide a smooth perception of the current evolution-related phenomena. Thus, for a maximum current frequency of 0.2 Hz, a DA throughput of 10 S/s was required. With these AD/DA constraints and the need for two input channels (EMF, Z) and four output channels (U, V, W1, and W23 current set points), a set of two BTH-1208LS boards from Measurement Computing (Newbury, United Kingdom) were chosen, taking into account the already growing experience that was being achieved in their use [30]. Direct connection of the search coil to one analog input (AI) was feasible due to its peak voltage being under 2 V. The optical encoder Z signal was connected to the other AI through a low-pass RC filter to widen the very thin encoder Z pulses so they could be detected using a 25 kS/s sampling rate. The ±2.5 V output voltage range was used to appropriately adjust the gain of the winding current drivers.

3.4. User Interface

The following design decisions primarily focused on the SLA user interface (UI), for which a widely used platform was selected: a PC-based LabVIEW© virtual instrument. The

general aim of the UI design was to facilitate the establishment of correlations between the winding structure/excitation and the AMF. Thus, it was divided into three main areas: a static display of winding arrangements, a winding current management console (WCMC), and the AMF live display (AMFLD) area, as shown in Figure 5.

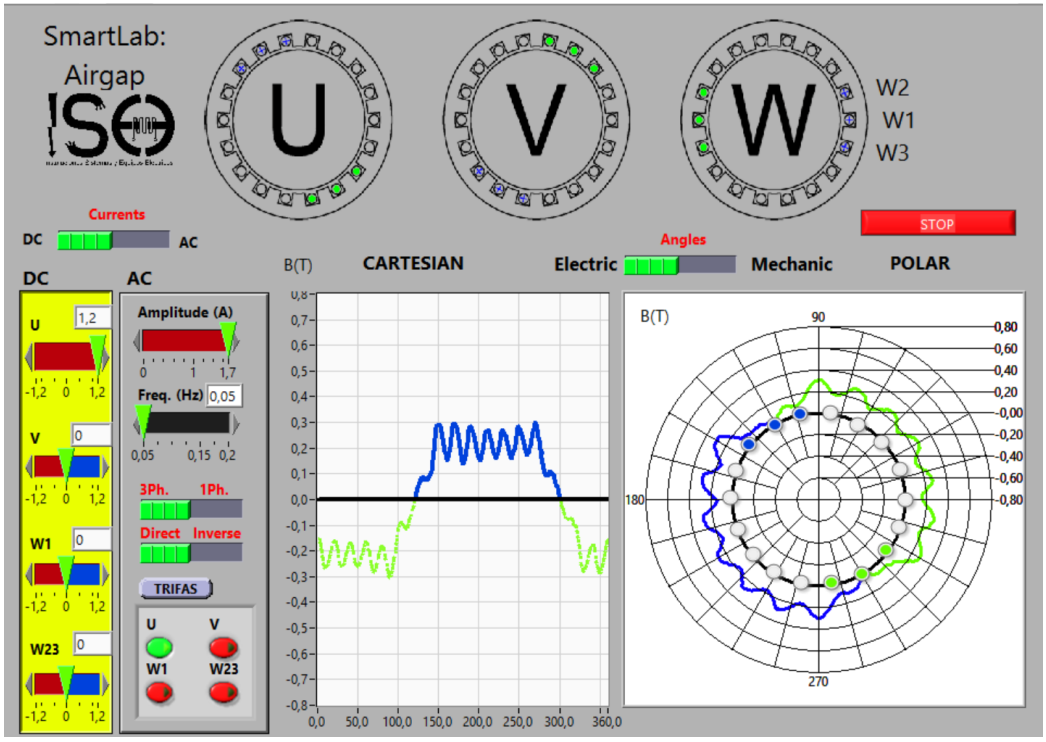


Figure 5. SmarLabAirgap user interface. Top left: VI identification with the name and iSEE research group logo. Top right: winding arrangement static display. Bottom left: winding current management console. Bottom right: AMF display in Cartesian and polar coordinates (blue—positive, green—negative color code). Single-phase operation in DC mode with only U phase winding positive current: AMF oriented at −150° (electrical).

The WCMC features a main selector to switch between DC and AC currents, along with two distinct areas dedicated to each mode. In the DC mode, users can individually adjust the current in any winding using slider controls, and all four windings can be operated simultaneously. In the AC mode, the main selector allows for switching between single-phase or three-phase operation, while two slider controls adjust the AC current amplitude and frequency. For single-phase operation, four mutually exclusive buttons enable the users to select the excited winding. In the three-phase operation, a selector permits the users to choose between direct or inverse phase sequences.

The AMFLD area was split into a Cartesian and polar representation of the indirectly measured AMF to help the user correlate the classic Cartesian representation of the AMF, most commonly used in text books, with the actually cylindrical air gap. To improve this correlation, the same color code (blue—positive, green—negative) was used in both Cartesian and polar graphs. The color-coded polar representation provides the user with a lasting image of the AMF in which the positive and negative magnetic poles and the field orientation can be easily identified and recognized. Furthermore, the WCS has also been included, with the same color code in the polar graph enriching the connection between the winding structure and the AMF waveform.

However, and to a great extent, the most outstanding feature of the color-coded polar representation is the ability to provide, through the live sequence of AMF states with AC current excitation, an easily identifiable description of the pulsating (single-phase AC) and rotating (three-phase AC) AMF to be compared to the stationary and constant AMF of

DC excitation [31]. The most descriptive features (pulsation or rotation frequency and amplitude) of this live display of the pulsating or rotating AMF can also be easily and directly linked to the excitation current frequency and amplitude just by adjusting the amplitude and frequency references to the WCMC. Finally, an electric/mechanic angle selector has been included to toggle between both representations of the AMF (an equivalent two pole or the four-pole structure of the actual electrical machine).

3.5. Instructional Guide

The instructional design to be followed by the users when working with the SLA is based on a step-by-step principle that facilitates a gradual comprehension and integration of the complex relationships between winding structure, excitation, and the AMF amplitude, waveform, orientation, and pulsation or rotation frequency.

The procedure starts with the simplest AMF produced by a concentrated full-pitch coil (W1) and then by two pitched coils (W23) with DC current. The user must recognize how the AMF amplitude is directly linked to the winding current, but the AMF orientation stays locked at 90° (electrical). Then, the windings U and V must be excited in turn to observe the shift in AMF orientation by ±120° (electrical), while the AMF amplitude is again linked to the phase current. At this point, two basic concepts must be recognized: first, that a winding fed by constant current produces an AMF whose orientation is fixed with respect to the winding and whose amplitude is directly related to the winding current, and second, that the use of distributed windings contributes to the AMF harmonics reduction.

The next step uses single-phase AC current with an adjustable amplitude and frequency on the different stator windings to always obtain a pulsating AMF whose orientation stays fixed to the excited winding. The user must then explore the effects of changing the current amplitude and frequency. Finally, the user must change to three-phase AC excitation to immediately observe how the AMF starts rotating. Three additional notions must be highlighted at this stage: first, the two-pole or four-pole AMF representation depending on the use of electrical or mechanical angles (compare Figures 6 and 7); second, how the four-pole real wave in the machine air gap actually rotates at half the angular frequency of the two-pole equivalent AMF wave in electrical degrees; and third, how the combined contribution of the three machine phases produces an AMF with a noticeably lower harmonic content.

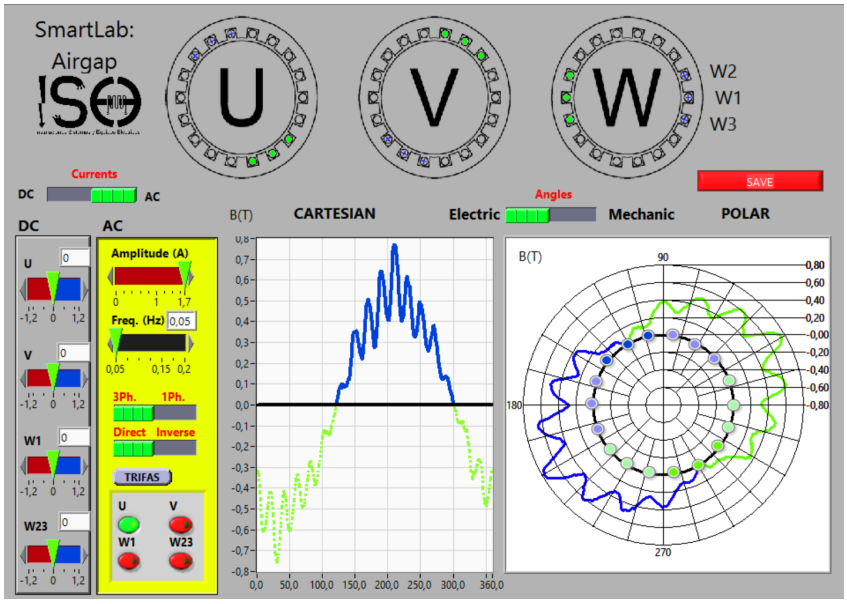


Figure 6. SmarLabAirgap with AC three-phase excitation: fairly sinusoidal rotating AMF with slotting effects.

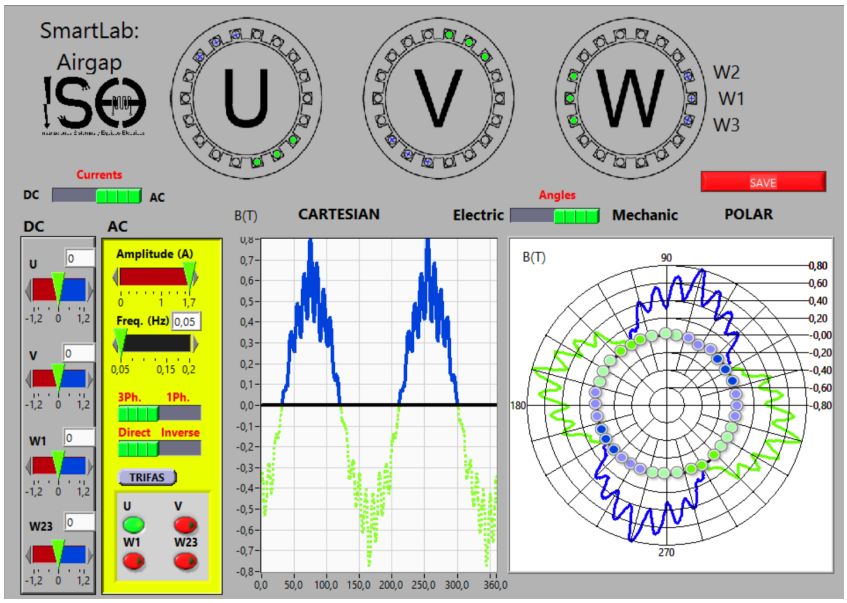


Figure 7. SmarLabAirgap with AC. Three-phase excitation and representation in geometrical degrees: four pole AMF that rotates at half the speed, calculated in electrical degrees.

3.6. Development of the Lab Session

The scope of our intervention focus is related to one of the twelve classroom sessions that make up the total student–instructor classroom contact over the rotating electrical machines part of the subject. In the second classroom session, the instructor and students work to theoretically understand the main connections between the current properties (amplitude, frequency) and winding distribution (location, distribution), along with the properties of the air gap magnetic field they produce together. These learning outcomes are reinforced in the lab session described above and are based on four experiments:

- Excitation with constant current in a single phase/coil/set of coils to see the link between current amplitude and phase/coil/coil set location, along with the field amplitude and orientation, noting that the air gap magnetic field is always constant in amplitude and in orientation.
- Excitation with single-phase alternating current to observe a pulsating magnetic field and to perceive the link between the current amplitude (max. value) and phase/coil/coil set location with the field pulsation amplitude and field orientation.
- Excitation with a sequence of constant phase currents corresponding to a three-phase sequence with an amplitude of 1 A and a frequency of 50 Hz at instants 0, 1, 2, 3, 4, and 5 ms. Each of these six time instants is experimented on its own; therefore, the phase currents for each instant are set to the phases, and the magnetic field produced by the combination is recorded in amplitude and orientation. When all instants have been recorded, the instructor calls attention to the fact that the sequence of three-phase currents produces a magnetic field with a constant amplitude across all time instants, and the orientation gradually changes at a rate of 18 electrical degrees per millisecond, corresponding to a current frequency of 50 Hz.
- Excitation with a three-phase alternating current is used to perceive the link between the current amplitude and field amplitude to perceive the 'rotation with constant amplitude' of the magnetic field and to link the frequency with the field rotating speed. To achieve this last objective, students are instructed to start a chronometer when the field is at a given position (e.g., pointing upwards) and then to stop it when the field completes one full rotation, appearing upwards again. This allows them to easily correlate the field rotation period with the current frequency and period.

This lab session is complemented with the no-load, locked-rotor, and load tests of the machine, with a total duration of 3 h. Continuing with the description of the curriculum

in the REM part of the course, this classroom session 2 is preceded by one introduction session to induction machines, where the main operational aspects are presented and worked on, as well as the two main constructive types, cage and wound rotor, together with their advantages, disadvantages, and main application areas. The session is followed by two sessions focused on obtaining the equivalent circuit and two sessions devoted to the applications of the equivalent circuit to the determination of the current, torque, and efficiency vs. speed curves. The last six classroom sessions are divided into halves and cover parameter identification using tests and manufacturer data, adjustable frequency operation (converter-fed machines), and the control objectives and criteria for operations below and above base speed.

4. Evaluation

SmartLabAirgap was introduced in all GITI, GIE, and MII Electrical Machines laboratory groups. The course was followed during this study by roughly 350 students per year. Its effectiveness was initially assessed based on a pre- and post-lab exam after the lectures. Before the laboratory began, and then again after the laboratory, a student survey was administered Finally, the average grade of the theory exam taken by the students at the end of the semester was calculated. The first two assessments were conducted only in some of the laboratory sessions during the first year due to the significant time required to take the exams and complete the survey, with a total of 79 students. The only statistic variables considered where the percentage of correct answers and their average for the pre/post lab exams. This study considers only the multiple-choice questions (which were designed to assess the attainment level of conceptual rather than procedural learning outcomes) for the rotating electrical machines part of the course. As a statistic variable, only the average grade was considered.

The pre- and post-lab exams had four multiple-choice questions covering the learning objectives. Figure 8 summarizes the results. Clearly, the laboratory contributed to improving the students' learning: the average grade (Q.Avg) increased by 27% from the baseline to close to 60% (the lab was conducted after the classroom lessons). The increase in the average mark for the individual questions ranged from 22% to 34% (the latter being for the question found to be the hardest before the lab). While this increase in the average grade cannot be solely ascribed to the new laboratory setup, it can be said to have had a positive impact on student learning.

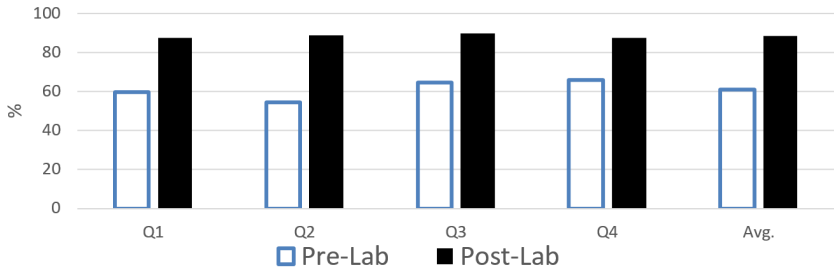


Figure 8. Pre- and post-laboratory exam results: Average % grade for all students taking the exams for all four Q1–Q4 questions and average exam grade.

The student satisfaction survey had five statements with a five-point scale, ranging from 1 (completely agree) to 5 (completely disagree):

S1. This laboratory was useful for your education on electrical machines.
S2. This laboratory helped you to understand concepts and enabled you to apply them in the topic being studied.
S3. This laboratory provided you with useful experience that might be of service in your future job.
S4. The educational materials used in this laboratory were adequate for the tasks to be performed.

S5. This laboratory increased your motivation to learn electrical machines.

The results of this survey, summarized in Figure 9, indicate a high level of student satisfaction with the laboratory. The responses predominantly ranged from 'completely agree' to 'agree'. The best scores were for statements S1 (usefulness), S2 (aid in understanding and applicability), and S4 (adequacy of the materials), all with nearly 90% of responses being between 'completely agree' and 'agree'.

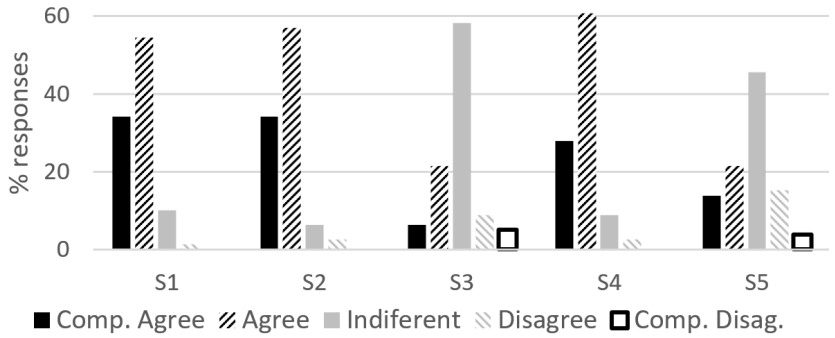


Figure 9. Student satisfaction survey responses to statements S1 to S5.

Finally, the introduction of the SLA in the laboratory sessions for all GITI and GIE groups demonstrated a clear impact on the student grades, as shown in Figure 10. This figure compares the results from the half-course multiple choice question exam recorded during the year prior to the introduction of the SmartLabAirgap to the students (Course 1 in Figure 10) and during the two years following the introduction of the SmartLabAirgap to the students (Course 2 and Course 3 in Figure 10). The difference illustrates that integrating the SmartLabAirgap to the learning schedule of the students had a positive impact on the subject grades, which must be linked to a positive impact on student learning.

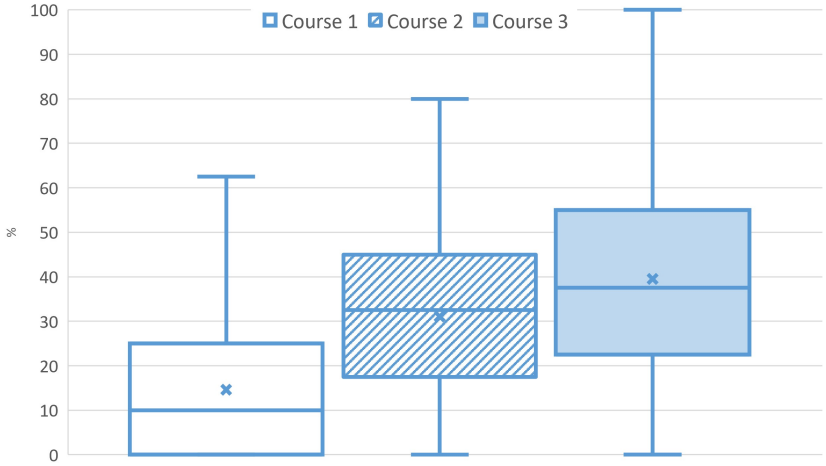


Figure 10. REM conceptual multiple-choice exam results throughout the 3 courses.

The students sat two exams (half semester—transformers and end of semester—REM), each one made up of 2 problems (62%) and 10 conceptual multiple-choice questions (38%). This last REM multiple-choice exam was deemed to better reflect the contribution of SLA to the intended objectives, as the problem grades were more related to procedural abilities rather than conceptual learning.

The exams each included a set of ten multiple-choice questions that were related to basic and more advanced topics within the rotating electrical machines subject. Therefore, the fact that the results showed a clear improvement may indicate that a better understanding of the basic rotating electrical machines' operational facts considered in the framework

of the SmartLabAirgap has helped to develop a better attainment of the course learning objectives in general terms.

5. Conclusions

A new test equipment apparatus complemented with a comprehensive set of laboratory experiments has been developed to address the learning challenges associated with the air gap magnetic field (AMF) of rotating electrical machines. The most important among these learning difficulties is the relationship between winding structure, exciting current, and AMF waveform properties like orientation, amplitude, and shape. Specially, the rotating magnetic field of three-phase AC machines and the relationship between its amplitude and angular velocity and the AC current frequency and amplitude are discussed. This new set, the SmartLabAirgap, enables the students to visualize the 'live' AMF of a real electrical machine for several winding configurations (full-pitched coil, two-pitched coils, and distributed windings with three slots per phase per pole) under different current excitations (adjustable DC, adjustable amplitude, and very low frequency single and three-phase AC).

Based on a survey, the SLA has been shown to result in high levels of student satisfaction, thus improving their motivation. The laboratory work significantly increased student abilities, as reflected in the exam results. Both evaluation elements, the survey and the exams, demonstrate that the main objectives set during the laboratory design phase were achieved.

As part of future work, there are plans to develop a simplified version based on a microcontroller and a modified squirrel cage machine. This approach aims to reduce the complexity and cost while maintaining the equipment's utility and effectiveness.

Author Contributions: Conceptualization, A.S.-B. and J.M.-R.; methodology, A.S.-B. and C.T.-S.; software, J.B.-V. and J.M.-R.; validation, A.S.-B. and J.B.-V.; formal analysis, J.B.-V. and C.T.-S.; investigation, A.S.-B. and C.T.-S.; resources, J.M.-R.; writing—original draft preparation, C.T.-S. and J.B.-V.; writing—review and editing, C.T.-S. and J.M.-R.; supervision, J.M.-R. and J.B.-V.; project administration, A.S.-B.; funding acquisition, A.S.-B. All authors have read and agreed to the published version of the manuscript.

Funding: This research has been funded by Universitat Politècnica de València within the framework of the Aprendizaje + Docencia: Proyectos de Innovación y Mejora Educativa program, A + D PIME 2021, with reference 1781, Desarrollo de competencias en diseño de Instalaciones Eléctricas de Baja Tensión mediante Aprendizaje Basado en Proyectos.

Conflicts of Interest: The authors declare no conflicts of interest.

Abbreviations

The following abbreviations are used in this manuscript:

AC	Alternating current
AD	Analog-to-digital
AI	Analog input
AMF	Airgap magnetic field
AMFLD	Airgap magnetic field display area
DA	Digital-to-analog
DAQ	Data acquisition systems
DC	Direct current
EMF	Electromotive force
GIE	Bachelor's Degree in Energy Engineering
GITI	Bachelor's Degree in Industial Engineering
IM	Induction machine
MII	Master's Degree in Industrial Engineering
REM	Rotating electrical machine
SL	SmartLab

SLA	SmartLabAirgap
UI	User interdace
VI	Virtual instrument
WCMC	Winding current management console
WCS	Winding current sheet

References

1. Nasar, S.A.; Unnewehr, L.E. *Electromechanics and Electric Machines*; John Wiley & Sons: Hoboken, NJ, USA, 1983.
2. Say, M. *Alternating Current Machines*, 5th ed.; John Wiley & Sons: Hoboken, NJ, USA, 1983.
3. Fitzgerald, A.E.; Kingsley, C.; Umans, S.D.; James, B. *Electric Machinery*; McGraw-Hill New York: New York, NY, USA, 2003; Volume 5.
4. Chapman, S. *Electric Machinery Fundamentals*; Tata McGraw-Hill Education: New York, NY, USA, 2005.
5. Pulijala, V.; Akula, A.R.; Syed, A. A web-based virtual laboratory for electromagnetic theory. In Proceedings of the 2013 IEEE Fifth International Conference on Technology for Education (T4E), Kharagpur, India, 18–20 December 2013; IEEE: Piscataway, NJ, USA, 2013; pp. 13–18.
6. Bentz, S. Integration of basic electromagnetism and engineering technology. In Proceedings of the Frontiers in Education Conference, 1995, Atlanta, GA, USA, 1–4 November 1995; IEEE: Piscataway, NJ, USA, 1995; Volume 2, pp. 4a5.4–4a5.7.
7. Gruber, S.; Prole, A. Measurement of Rotating Air Gap Magnetic Fields-An Undergraduate Laboratory Experiment. *IEEE Trans. Educ.* **1979**, *22*, 143–145. [CrossRef]
8. Ueda, Y.; Ohta, H.; Uenosono, C. Instrument for real-time measurements of airgap flux distribution of on-load synchronous generators. *IEE Proc.-Phys. Sci. Meas. Instrum. Manag.-Educ.-Rev.* **1987**, *134*, 331–334. [CrossRef]
9. Smolleck, H. A simple revolving-field demonstrator for the Personal Computer. *IEEE Trans. Educ.* **1988**, *31*, 119–123. [CrossRef]
10. Akbaba, M. Teaching transient behavior of electrical machines with personal computers. *Comput. Educ.* **1997**, *28*, 155–164. [CrossRef]
11. Ojaghi, M.; Faiz, J.; Kazemi, M.; Rezaei, M. Performance analysis of saturated induction motors by virtual tests. *IEEE Trans. Educ.* **2012**, *55*, 370–377. [CrossRef]
12. Iqbal, A.; Singh, G.K. Virtual Laboratory to Conduct Slip Test of Synchronous Machine. *i-Manag. J. Sch. Educ. Technol.* **2021**, *17*, 11.
13. Lei, Z.; Zhou, H.; Hu, W.; Deng, Q.; Zhou, D.; Liu, Z.W.; Gao, X. 3-D interactive control laboratory for classroom demonstration and online experimentation in engineering education. *IEEE Trans. Educ.* **2020**, *64*, 276–282. [CrossRef]
14. Potkonjak, V.; Vukobratović, M.; Jovanović, K.; Medenica, M. Virtual Mechatronic/Robotic laboratory—A step further in distance learning. *Comput. Educ.* **2010**, *55*, 465–475. [CrossRef]
15. Rahman, I.; Johari, M. Students' understanding and skills on voltage and current measurements using hands-on laboratory and simulation software. *Educ. Inf. Technol.* **2022**, *27*, 6393–6406. [CrossRef]
16. Potkonjak, V.; Gardner, M.; Callaghan, V.; Mattila, P.; Guetl, C.; Petrović, V.M.; Jovanović, K. Virtual laboratories for education in science, technology, and engineering: A review. *Comput. Educ.* **2016**, *95*, 309–327. [CrossRef]
17. Chang, H.Y.; Binali, T.; Liang, J.C.; Chiou, G.L.; Cheng, K.H.; Lee, S.W.Y.; Tsai, C.C. Ten years of augmented reality in education: A meta-analysis of (quasi-) experimental studies to investigate the impact. *Comput. Educ.* **2022**, *191*, 104641. [CrossRef]
18. Ibáñez, M.B.; Di Serio, Á.; Villarán, D.; Kloos, C.D. Experimenting with electromagnetism using augmented reality: Impact on flow student experience and educational effectiveness. *Comput. Educ.* **2014**, *71*, 1–13. [CrossRef]
19. Martinez-Roman, J.; Perez-Cruz, J.; Pineda-Sanchez, M.; Puche-Panadero, R.; Roger-Folch, J.; Riera-Guasp, M.; Sapena-Baño, A. Electrical machines laminations magnetic properties: A virtual instrument laboratory. *IEEE Trans. Educ.* **2015**, *58*, 159–166. [CrossRef]
20. Gruber, S. A computer-interfaced electrical machines laboratory. *IEEE Trans. Educ.* **1984**, *27*, 73–79. [CrossRef]
21. Williams, J.M.; Cale, J.L.; Benavides, N.D.; Wooldridge, J.D.; Koenig, A.C.; Tichenor, J.L.; Pekarek, S.D. Versatile hardware and software tools for educating students in power electronics. *IEEE Trans. Educ.* **2004**, *47*, 436–445. [CrossRef]
22. Jimenez-Martinez, J.M.; Soto, F.; de Jódar, E.; Villarejo, J.A.; Roca-Dorda, J. A new approach for teaching power electronics converter experiments. *IEEE Trans. Educ.* **2005**, *48*, 513–519. [CrossRef]
23. Sellschopp, F.S.; Arjona, L.M.A. An automated system for frequency response analysis with application to an undergraduate laboratory of electrical machines. *IEEE Trans. Educ.* **2004**, *47*, 57–64. [CrossRef]
24. Dak, R.; Khoje, S.; Pardeshi, P.J. A review on cost-efficient virtual laboratory: A teaching aid. In Proceedings of the 2017 International Conference on Computing Methodologies and Communication (ICCMC), Erode, India, 18–19 July 2017; IEEE: Piscataway, NJ, USA, 2017; pp. 663–667.
25. Fernandez, R.M.; Garcia-Loro, F.; Alves, G.; López-Rey, A.; Meier, R.; Castro, M. New scenarios and trends in non-traditional laboratories from 2000 to 2020. *IEEE Trans. Learn. Technol.* **2024**, *17*, 1568–1587. [CrossRef]
26. Dal, M. Teaching electric drives control course: Incorporation of active learning into the classroom. *IEEE Trans. Educ.* **2013**, *56*, 459–469. [CrossRef]
27. Duran, M.J.; Barrero, F.; Pozo-Ruz, A.; Guzman, F.; Fernandez, J.; Guzman, H. Understanding power electronics and electrical machines in multidisciplinary wind energy conversion system courses. *IEEE Trans. Educ.* **2013**, *56*, 174–182. [CrossRef]

28. Heath, W.; Onel, O.; Green, P.; Lennox, B.; Gai, Z.; He, Z.; Liñan, M.R. Developing a Student-Focused Undergraduate Laboratory. *Int. J. Electr. Eng. Educ.* **2013**, *50*, 268–278. [CrossRef]
29. Bujanovic, T.; Ghosh, P. Laboratory experiments for enhanced learning of electromechanical devices. In Proceedings of the 2014 Zone 1 Conference of the American Society for Engineering Education (ASEE Zone 1), Bridgeport, CT, USA, 3–5 April 2014; IEEE: Piscataway, NJ, USA, 2014; pp. 1–5.
30. Martinez-Roman, J.; Tarin-Corachan, J.; Perez-Cruz, J.; Pineda-Sanchez, M.; Puche-Panadero, R.; Sapena-Baño, A.; Guasp, M.R.; Folch, J.R. Dynamizing electrical machines laboratories with virtual instruments: The UPV experience. In Proceedings of the 2014 International Conference on Electrical Machines (ICEM), Berlin, Germany, 2–5 September 2014; IEEE: Piscataway, NJ, USA, 2014; pp. 137–143.
31. ISEE (Instalations Systems and Electrical Equipment) UPV, 'Smartlab Airgap Demo Videoclip'. Available online: https://media.upv.es/player/?id=44735390-2d5a-11ef-91f5-4fcf8248fca3 (accessed on 7 July 2024).

Disclaimer/Publisher's Note: The statements, opinions and data contained in all publications are solely those of the individual author(s) and contributor(s) and not of MDPI and/or the editor(s). MDPI and/or the editor(s) disclaim responsibility for any injury to people or property resulting from any ideas, methods, instructions or products referred to in the content.